

AUTOPEFT: Automatic Configuration Search for Parameter-Efficient Fine-Tuning

Han Zhou^{1*} Xingchen Wan^{2*} Ivan Vulic¹ Anna Korhonen¹

¹Language Technology Lab, University of Cambridge

²Machine Learning Research Group, University of Oxford

{hz416, iv250, alk23}@cam.ac.uk

xwan@robots.ox.ac.uk

Abstract

Large pretrained language models have been widely used in downstream NLP tasks via task-specific fine-tuning. Recently, an array of Parameter-Efficient Fine-Tuning (PEFT) methods have also achieved strong task performance while updating a much smaller number of parameters compared to full model tuning. However, it is non-trivial to make informed *per-task* design choices (i.e., to create *PEFT configurations*) concerning the selection of PEFT architectures and modules, the number of tunable parameters, and even the layers in which the PEFT modules are inserted. Consequently, it is highly likely that the current, manually set PEFT configurations might be suboptimal for many tasks from the perspective of the performance-to-efficiency trade-off. To address the core question of the PEFT configuration selection that aims to control and maximise the balance between performance and parameter efficiency, we first define a rich configuration search space spanning multiple representative PEFT modules along with finer-grained configuration decisions over the modules (e.g., parameter budget, insertion layer). We then propose AUTOPEFT, a novel framework to traverse this configuration space: it **automatically** configures multiple **PEFT** modules via high-dimensional Bayesian optimisation. We show the resource scalability and task transferability of AUTOPEFT-found configurations, outperforming existing PEFT methods on average on the standard GLUE benchmark while conducting the configuration search on a single task. The *per-task* AUTOPEFT-based configuration search even outperforms full-model tuning.

1 Introduction and Motivation

Pretrained language models (PLM) are used in downstream tasks via the standard transfer learning

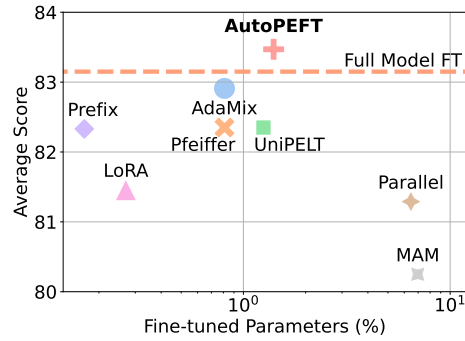


Figure 1: The performance of AUTOPEFT-found PEFT configurations compared to other standard PEFT methods and full model FT on the GLUE benchmark (Wang et al., 2018). We report the average score for each method by taking the mean of metrics for 8 GLUE tasks. The dashed horizontal bar (*Full Model FT*) indicates the full-model FT that updates 100% of parameters, and our approach aims to learn the best trade-off configuration between task performance and parameter efficiency.

paradigm, where they get fine-tuned for particular tasks (Devlin et al., 2019; Liu et al., 2019b). This achieves state-of-the-art results in a wide spectrum of NLP tasks, becoming a prevalent modelling paradigm in NLP (Raffel et al., 2020). Fine-tuning the PLMs typically requires a full update of their original parameters (i.e., the so-called *full-model fine-tuning (FT)*); however, this is (i) computationally expensive and also (ii) storage-wise expensive as it requires saving a separate full model copy for each task-tuned model. With the ever-growing size of the PLMs (Brown et al., 2020; Sanh et al., 2022), the cost of full model FT becomes a major bottleneck, due to its increasing demands as well as computational (time and space) non-efficiency.

Parameter-Efficient Fine-Tuning (PEFT) delivers a solution for alleviating the issues with full-model FT (Houlsby et al., 2019). By freezing the majority of pretrained weights of PLMs, PEFT approaches only update a small portion of parameters

*Equal contribution. Code is available at <https://github.com/cambridgeltl/autopeft>

for efficiently adapting the PLM to a new downstream task. Recent studies have shown that PEFT can achieve competitive task performance while being modular, adaptable, and preventing catastrophic forgetting in comparison to traditional FT (Wang et al., 2022).

Recent developments have created diverse PEFT modules with distinctive characteristics (Pfeiffer et al., 2020b; Li and Liang, 2021), with one of the two main aims in focus: **1)** *improve task performance over other PEFT approaches while maintaining the same parameter budget* as the competitor PEFT methods; or **2)** *maintain task performance while reducing the parameter budget* needed. Existing PEFT modules, optimising for one of the two aims, have been successfully applied to transfer learning tasks (Chen et al., 2022b; Pfeiffer et al., 2022). However, different tasks, with different complexity, show distinct sensitivity to the allocated parameter budget and even to the chosen PEFT approach (He et al., 2022). At the same time, most PEFT applications are limited to a single PEFT architecture (e.g., serial adapters, prefix-tuning) with fixed decisions on its components (e.g., hidden size dimensionality, insertion layers) resulting in *potentially suboptimal PEFT configurations* across many tasks. Therefore, in this work, we propose a new, versatile and unified framework that automatically searches for improved and task-adapted PEFT configurations, aiming to *effectively balance* between the two (often colliding goals) of (i) improving performance and (ii) keeping the desired low parameter budget for PEFT.

While recent research has started exploring more dynamic PEFT configurations, the prior studies remain limited across several dimensions, including how they define the configuration search space. Namely, they typically focus only on a single PEFT architecture (e.g., adapters) or their simple combinations, or a single property (e.g., insertion layers – where to insert the module); see a short overview later in §2. Here, we propose a unified and more comprehensive framework for improved configuration search. It covers multiple standard PEFT modules (1. serial adapters, 2. parallel adapters, 3. prefix-tuning), combined with the critical parameter budget-related decisions: the size of each constituent module and the insertion layers for the modules.

Our defined comprehensive search space is huge; as a consequence, traversing it effectively *and* effi-

ciently is extremely challenging. To enable search over the large configuration space, we thus propose the AUTOPEFT framework. It **automatically** configures multiple **PEFT** modules along with their efficiency-oriented design decisions, relying on a high-dimensional Bayesian optimisation (BO) approach. Crucially, within the search space, we propose a multi-objective optimisation which learns to simultaneously balance between maximising the searched configurations’ task performance *and* parameter efficiency.

We conduct extensive experiments on the standard GLUE benchmark (Wang et al., 2018). We first study the transferability of the AUTOPEFT-searched architecture by running AUTOPEFT on a single task, followed by transferring the found architecture to other tasks. Experimental results show that this architecture can outperform existing PEFT baselines while achieving on-par performance to the standard full-model FT, relying only on 1.4% of the original trainable parameters. Further slight gains can be achieved via a computationally more expensive approach, where we run AUTOPEFT per each single task to find a task-adapted PEFT configuration. As demonstrated in Figure 1, AUTOPEFT is able to find configurations that offer a solid trade-off between task performance and parameter efficiency, even outperforming full-model FT. We also provide ablation studies over the search space, validating that the AUTOPEFT framework is versatile and portable to different search spaces.

Contributions. **1)** We propose a large and comprehensive search space of PEFT configurations, which integrates three representative PEFT modules, the tunable number of parameters of each module, and the binary decisions concerning Transformer layers for inserting these modules. **2)** We propose a novel AUTOPEFT framework with high-dimensional Bayesian optimisation that can automatically and feasibly search for the effective PEFT configuration in terms of both task performance and parameter efficiency. **3)** We demonstrate that the AUTOPEFT-found configurations can not only reduce the parameter budget but also outperform existing PEFT modules while being transferable across tasks. The AUTOPEFT framework can also be easily extended to other and new PEFT modules.

2 Related Work

Parameter-Efficient Fine-Tuning. Standard PEFT methods can be divided into two main

groups. **1)** Some methods fine-tune a small portion of pretrained parameters (Zhao et al., 2020; Guo et al., 2021). For instance, Ben Zaken et al. (2022) propose to fine-tune the PLM’s bias terms, while Sung et al. (2021) and Ansell et al. (2022) fine-tune sparse subnetworks withing the original PLM for a particular task. **2)** Other methods fine-tune an additional set of parameters (Liu et al., 2022). Since there is no interference with the pretrained parameters, this class of PEFT modules, besides offering strong task performance, is arguably more modular; we thus focus on this class of PEFT methods in this work. The original *adapter modules* (Houlsby et al., 2019; Pfeiffer et al., 2020b) have a bottleneck *serial* architecture which can be inserted into every Transformer layer, see Figure 2. LORA (Hu et al., 2022a) assumes the low-rank intrinsic dimensionality of the target task and performs low-rank updates (Mahabadi et al., 2021). Li and Liang (2021) propose the Prefix-Tuning method that appends a learnable vector to the attention heads at each Transformer layer. Similarly, prompt-tuning (Lester et al., 2021) only appends this vector to the input embedding. UniPELT (Mao et al., 2022) integrates multiple PEFT modules with a dynamic gating mechanism. He et al. (2022) provide a unified formulation of existing PEFT modules and propose a *parallel* adapter module, along with a combined ‘Mix-and-Match Adapter (MAM)’ architecture that blends parallel adapters and prefix-tuning. Wang et al. (2022) propose the mixture-of-adaptations (AdaMix) combined architecture that leverages weight averaging for a mixture of adapters.

Optimising Parameter Efficiency in PEFT. Recent work further aims to optimise the parameter efficiency of existing PEFT modules while maintaining task performance. The standard approach is to insert (typically serial) adapters into all Transformer layers, which still requires a sizeable parameter budget. Rücklé et al. (2021) address this question by performing random dropout of adapters from lower-level layers, displaying only a small decrease in task performance. Adaptable Adapters (AA) (Moosavi et al., 2022) generalise this idea by learning gates that switch on or off adapters in particular Transformer layers. Neural Architecture Search (NAS) methods aim to automate the design of neural net architectures themselves, and NAS has seen great advances recently, with performance often surpassing human expert-designed

architectures in various tasks (Zoph and Le, 2017; Ren et al., 2021; Elsken et al., 2019). Concerning NLP tasks and PEFT, Hu et al. (2022b) propose S₃PET, which adapts Differentiable Architecture Search (DARTS) (Liu et al., 2019a) to learn the positions for inserting the PEFT modules. This work is closest in spirit to ours.

Our method, discussed in detail in §3, offers a spectrum of advantages over S₃PET and other related PEFT work. Relying on multi-objective optimisation, unlike S₃PET, we can automatically discover a family of configurations at different parameter efficiency levels in a single search run, effectively balancing between task performance and parameter efficiency, without the need to set the ‘parameter budget’ in advance; similarly, we enable an automatic search over multiple constituent modules over the desirable range of parameter budget and effective layers, whereas previous work can only support one architecture per each search run. Further, previous work indicated that weight-sharing NAS such as DARTS may suffer with the reliability of prediction (White et al., 2021b), and its success often hinges heavily on the design of the actual *search space* (Li and Talwalkar, 2019; Ru et al., 2020; Dong and Yang, 2020; Yang et al., 2020). We mitigate those issues with our design of AUTOPEFT. Finally, while weight-sharing NAS is arguably more computationally efficient, through combining the use of low-fidelity performance predictors and the strong transferability of the configurations found across tasks, AUTOPEFT can also be made very computationally efficient in discovering effective PEFT configurations. We further discuss this in §3 and demonstrate empirically in §5.

3 AUTOPEFT Framework

We start by designing a large configuration space, providing the motivation behind each decision to include a particular module and its components into the configuration space, along with a mathematical formulation. We then propose AUTOPEFT, a novel framework to search over this challenging configuration space. It automatically configures (components of) multiple **PEFT** modules via high-dimensional Bayesian optimisation.

PEFT Configuration Search Space. The search space is an influential factor in the performance of any search algorithm. In order to simultaneously maximise task performance along with parameter efficiency, it is necessary to first define a

‘parameter-reducible’ search space, where each dimension within the space potentially contributes to reducing the parameter budget. Similarly, each dimension might potentially bring positive impact to the task performance without introducing redundancy in the space (Wan et al., 2022). Therefore, we propose the search space with representative PEFT modules, as follows, spanning a plethora of (non-redundant) configurations, as also shown in Figure 2.

PEFT Modules. We include three distinctive PEFT designs to efficiently adapt different forwarding stages of hidden states in the PLM layers. We combine Serial Adapters (SA), Parallel Adapters (PA), and Prefix-Tuning (PT) as the three representative modules in the search space, where the PT module adapts the multi-head attention layer, and SA and PA interact with the FFN layer (Figure 2). Each configuration makes a decision on the PEFT modules in the insertion layer: all of them can be ‘turned’ on or off. We combine this binary decision with the actual non-binary decision on the module size (see next), so that the value of 0 in fact denotes the absence of the modules in the layer(s).

Size. Previous studies show that PEFT methods are highly sensitive to the number of tunable parameters: adaptively setting their capacity in accordance with the target task is then essential for achieving good performance (Chen et al., 2022a). The number of tunable parameters is dependent on each particular module. The additional parameters introduced by both SA and PA are dominated by their bottleneck dimension D . Similarly, the size of the PT module is defined by its prefix length L_{PT} . Thus, we define a binary logarithmic search scale for the respective discrete sets D_{SA} , D_{PA} , and L_{PT} , spanning the values from 0 (absence of the module) to D_h where D_h is the dimensionality of the PLM (e.g., $D_h=768$ for BERT_{base}).

Insertion Layers. Prior work has also shown that different layers in the PLMs store different semantic information (Vulić et al., 2020), where the higher layers produce more task-specific and contextualized representations (Tenney et al., 2019). Therefore, as another configuration dimension, we aim to search for the minimal number and the actual position of layers in which to insert the PEFT modules. We define a binary ‘insertion’ decision at each layer l_i .

Combining PEFT Modules. The SA module and the PA module share a bottleneck architecture. The

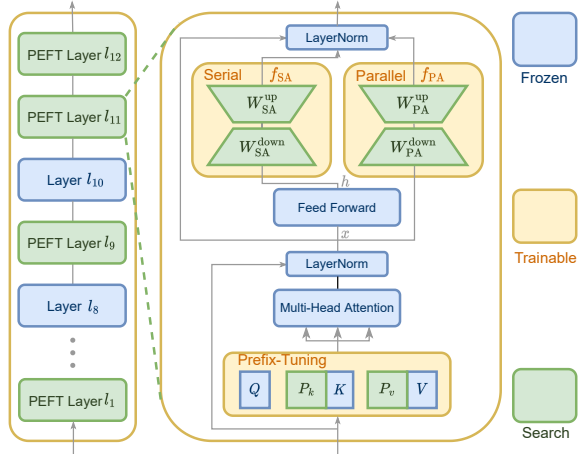


Figure 2: Illustration of the main components of our configuration search space, traversed via AUTOPEFT. AUTOPEFT configures the selected Transformer layers with PEFT modules, where the activation of each submodule is controlled by the learned size of each submodule. See also Table 4 in the appendix.

SA receives hidden states from the FFN output as its inputs, adapting it with a down-projection matrix $W_{SA}^{down} \in \mathbb{R}^{D_h \times D_{SA}}$, followed by a non-linear activation function, and then an up-projection matrix $W_{SA}^{up} \in \mathbb{R}^{D_{SA} \times D_h}$:

$$f_{SA}(h) = \text{ReLU}(hW_{SA}^{down})W_{SA}^{up}. \quad (1)$$

PA, on the other hand, receives its inputs from hidden states before the FFN layer with the same formulation:

$$f_{PA}(x) = \text{ReLU}(xW_{PA}^{down})W_{PA}^{up}. \quad (2)$$

Therefore, it is able to act in parallel with the SA without interference. Note that the FFN hidden states $h = F(x)$ contain the task-specific bias learned in its pretrained weights. Therefore, by combining SA with PA, the following composition of functions is achieved:

$$\begin{aligned} f_{SAPA}(x) = & \text{ReLU}(F(x)W_{SA}^{down})W_{SA}^{up} \\ & + \text{ReLU}(xW_{PA}^{down})W_{PA}^{up}. \end{aligned} \quad (3)$$

The final composition should provide an effective adaptation to both bias-influence hidden states and the original inputs before the pretrained FFN layer.¹

Further, applying PEFT modules to interact both with FFNs and multi-head attention should have a positive impact on task performance (Mao et al.,

¹The PA module also acts as the low-rank reparametrization of the learned SA together with the frozen FFN layer to further match the intrinsic dimensionality of the target task.

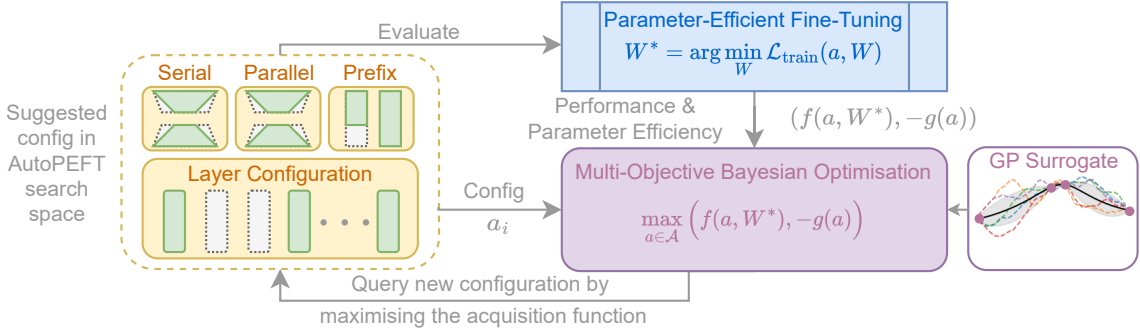


Figure 3: Illustration of the AUTOPEFT framework: to search for optimal architectures in the defined configuration space, AUTOPEFT uses a *multi-objective BO agent*, which trains on previous observations of the PEFT configuration vector and its performance (e.g., accuracy – obtained by fine-tuning the language model with the PEFT configuration) and cost (e.g., number of parameters). The BO agent then suggests new configurations, and the algorithm continues iteratively until convergence.

2022; He et al., 2022). PT learns two prefix vectors, P_k and $P_v \in \mathbb{R}^{L_{\text{PT}} \times D_h}$, that are concatenated with the original multi-head attention’s key and value vectors, which efficiently adapts the multi-head attention layer to fit the target task. We thus finally combine the SA and the PA (i.e., SAPA from above) with PT.

In sum, the overview of the dimensions spanning the final configuration space is provided in Figure 2 and Table 4. The combination of the different ‘configuration dimensions’ outlined above gives rise to a total of e.g., 5,451,776 possible configurations with BERT_{base} and $\sim 3 \times 10^{10}$ configurations with RoBERTa_{large} (i.e., the number of configurations is $2^{|l|} \times |D_{\text{SA}}| \times |D_{\text{PA}}| \times |L_{\text{PT}}|$). While a large search space is crucial for expressiveness and to ensure that good-performing configurations are contained, it also increases the difficulty for search strategies to both navigate the search space well while remaining sample- and thus computationally efficient. Furthermore, in the PEFT setting, we are also often interested in discovering a family of configurations that trade off between performance and efficiency for general application in various scenarios with different resource constraints, thus giving rise to a multi-objective optimisation problem where we simultaneously aim to maximise performance while minimising costs. In what follows, we propose a search framework that satisfies all those criteria.

AUTOPEFT via Multi-Objective Bayesian Optimisation. Formally, denoting the full AUTOPEFT search space as \mathcal{A} and a single configuration $a \in \mathcal{A}$ with trainable weights W , without loss of generality, assuming our objective is to maximise (i) a performance metric $f(a, W)$ (e.g., the accuracy

on the dev set) and to (ii) minimise a cost metric $g(a)$ (e.g., the number of parameters in a), a search method aims to solve the bi-level, bi-objective optimisation problem:

$$\begin{aligned} & \max_{a \in \mathcal{A}} (f(a, W^*), -g(a)); \\ & \text{s.t. } W^* = \arg \min_W \mathcal{L}_{\text{train}}(a, W), \end{aligned} \quad (4)$$

where the inner loop optimisation problem is the optimisation of the configuration *weights* achieved by fine-tuning the configuration a itself over the train loss $\mathcal{L}_{\text{train}}$. Given the bi-objective nature of the problem, there is in general no single maximiser of Eq. (4) but a *set* of non-dominated Pareto-optimal configurations $A^* = \{a_1^*, \dots, a_{|A^*|}^*\}$.

To address these challenges in this work, we adopt a Bayesian optimisation (BO) approach, illustrated in Figure 3. BO is a sample-efficient, zeroth-order model-based sequential optimisation algorithm (Garnett, 2023) with proven successes in NAS and automated machine learning in general (Snoek et al., 2012; White et al., 2021a; Ru et al., 2021; Kandasamy et al., 2018). BO is particularly popular in the multi-objective setups where one is interested in recovering a Pareto front where it is less straightforward to apply methods such as differentiable / one-shot architecture search methods that are typically used to discover a single best-performing configuration (Eriksson et al., 2021; Izquierdo et al., 2021). BO consists of a surrogate model, usually a Gaussian Process (GP) that sequentially approximates the objective function based on the observations so far, and an acquisition function, which balances between exploitation (i.e., regions in the search space with high perceived

value) and exploration (i.e., regions that have not been visited before). It is optimised at each iteration to actively select the next configuration to evaluate. For a detailed overview of BO, we refer the readers to [Frazier \(2018\)](#).

While vanilla BO methods are better-suited in modestly-dimensioned and continuous problems, our current setup instead features a high-dimensional and combinatorial search space. Here, performance of non-parametric methods such as GP-based BO tend to suffer due to the exponentially exploding volume of space the surrogate needs to model as dimensionality increases. Fortunately, recent advances in search methods have allowed us to address these challenges effectively. Specifically, we adopt the SAAS-GP ([Eriksson and Jankowiak, 2021](#)) model as the surrogate function: on a high level, SAAS-GP (1) places a relatively strong regularising half-Cauchy prior on the model lengthscales (which dictate the perceived importance of search dimensions to the objective function value) to induce sparsity and (2) approximately marginalises over model hyperparameters via a No-U-Turn Monte Carlo sampler ([Hoffman et al., 2014](#)) to reduce overfitting in high dimensions. We argue that both are appealing in our setup, while the benefit of (2) in our setup is self-evident, (1) also effectively places a prior to encode our belief that in spite of the high *nominal* complexity search space, the *effective* dimensionality of the problem should be much lower – this is appropriate in our setup, as although we have a nominally high dimensions, consistent to previous findings in NAS ([Wan et al., 2022](#)), we do expect a few disproportionately influential key dimensions (although we do not have information on *which* a priori – this is meant to be discovered by the BO algorithm).

For the acquisition function, we use the noisy expected hypervolume improvement (NE-HVI) ([Daulton et al., 2021](#)), which is suitable for the setup described in Eq. 4. Lastly, while BO is sample-efficient, it may still require 100-200 evaluations of different configurations in the search space to sufficiently explore the search space; to make sure the search remains cost-efficient, during search we also adopt *low-fidelity* approximations commonly employed in NAS: at the search stage, for a configuration a , instead of evaluating the objective $f(a, W)$ defined in Eq. 4 in full, we only fine-tune the a using a smaller computational budget – for example, if a complete fine-tuning takes

100% of training data, at search time we are able to only fine-tune with 1% of training data and use the accuracy after that as a lower-cost proxy to the accuracy after full-length FT, the latter of which is significantly more expensive to obtain. Therefore, when we are facing high-resource tasks, fine-tuning the full training resources is only performed once at evaluation time after the Pareto-optimal configurations are finalised. Other low-cost proxies such as training for fewer number of epochs than full FT are also compatible but not used in the present work.

4 Experimental Setup

Evaluation Data. We follow prior PEFT research and base our evaluation on the standard GLUE benchmark. We include 4 types of text classification tasks, including linguistic acceptability: CoLA; similarity and paraphrase: STS-B, MRPC, QQP; sentiment analysis: SST-2; natural language inference: RTE, QNLI, MNLI. We exclude WNLI following previous work ([Houlsby et al., 2019](#); [Mao et al., 2022](#)).

Baselines. We compare the performance of the AUTOPEFT-found configurations to the standard full model FT and each individual PEFT module (SA, PA, PT) from the search space used in their default setup from respective original work. We also compare with the LoRA module, to provide a comparison to low-rank decomposition methods. In order to provide comparisons with recently proposed methods that also integrate multiple PEFT modules (see §2), we further include the UniPELT and the MAM adapter in their default settings. We reproduce AdaMix for a comparison to a mixture of homogeneous adaptations. In ablations on insertion layers, we also include the Adaptable Adapter (AA) as a baseline that proposes a differentiable gate learning method to select the insertion layer for PEFT modules (i.e., serial adapters originally).

Implementation Details. Following previous work on the GLUE benchmark, we report the best GLUE dev set performance ([Ben Zaken et al., 2022](#)) and use 20 training epochs with an early stopping scheme of 10 epochs for all tasks. We use AdapterHub ([Pfeiffer et al., 2020a](#)) as the codebase and conduct extensive experiments with the uncased BERT_{base} ([Devlin et al., 2019](#)) as the main backbone model. We report main experiments with the mean and standard deviation over 5 different random seeds. Experimental results using

Method	#Param.	RTE	MRPC	STS-B	CoLA	SST-2	QNLI	QQP	MNLI	Avg.
Fine-tune	100%	71.12 _{1.46}	85.74 _{1.75}	89.00 _{0.45}	59.32 _{0.62}	92.57 _{0.24}	91.50 _{0.08}	91.52 _{0.04}	84.43 _{0.22}	83.15
Prefix	0.17%	70.54 _{0.49}	85.93 _{0.89}	88.76 _{0.15}	58.88 _{1.15}	91.93 _{0.45}	90.76 _{0.14}	89.12 _{0.07}	82.78 _{0.16}	82.33
LoRA	0.27%	65.85 _{1.49}	84.46 _{1.04}	88.73 _{0.08}	57.58 _{0.78}	92.06 _{0.38}	90.62 _{0.22}	89.41 _{0.04}	83.00 _{0.07}	81.46
Serial	0.81%	68.01 _{1.34}	84.75 _{0.45}	88.61 _{0.11}	59.73 _{0.62}	91.93 _{0.33}	91.06 _{0.12}	90.52 _{0.05}	84.18 _{0.22}	82.35
AdaMix	0.81%	70.11 _{0.62}	86.86 _{1.12}	89.12 _{0.11}	59.11 _{1.00}	92.06 _{0.22}	91.52 _{0.15}	90.22 _{0.04}	84.25 _{0.14}	82.91
UniPELT	1.25%	67.07 _{1.82}	84.22 _{0.78}	88.84 _{0.11}	60.13 _{0.46}	92.52 _{0.24}	91.09 _{0.13}	90.69 _{0.11}	84.28 _{0.18}	82.35
Parallel	6.46%	68.52 _{3.44}	86.52 _{0.96}	88.90 _{0.28}	58.72 _{1.69}	92.13 _{0.35}	90.83 _{0.22}	90.74 _{0.08}	73.93 _{19.24}	81.29
MAM	6.97%	69.10 _{1.76}	87.16 _{0.74}	89.01 _{0.48}	47.87 _{23.97}	83.94 _{16.52}	90.85 _{0.22}	90.76 _{0.05}	83.31 _{0.17}	80.25
AUTOPEFT ^{RTE} _S	0.06%	69.68 _{0.76}	85.54 _{0.78}	88.78 _{0.18}	56.83 _{0.54}	91.93 _{0.34}	90.81 _{0.18}	88.51 _{0.05}	82.26 _{0.11}	81.79
AUTOPEFT ^{MNLI} _S	0.30%	69.77 _{0.47}	85.73 _{0.61}	88.78 _{0.17}	57.50 _{1.79}	91.88 _{0.32}	91.12 _{0.13}	89.90 _{0.05}	83.92 _{0.10}	82.32
AUTOPEFT ^{RTE} _M	1.42%	72.35 _{0.84}	86.13 _{0.62}	89.06 _{0.09}	60.23 _{1.00}	92.11 _{0.23}	91.00 _{0.09}	90.64 _{0.07}	84.01 _{0.21}	83.19
AUTOPEFT ^{RTE} _L	6.60%	71.70 _{1.18}	86.62 _{0.65}	89.19 _{0.13}	59.44 _{0.75}	92.41 _{0.28}	91.09 _{0.12}	90.79 _{0.06}	83.91 _{0.14}	83.14
AUTOPEFT ^{task} _{Avg.}	1.40%	72.35 _{0.94}	87.45 _{0.87}	89.17 _{0.00}	60.92 _{1.47}	92.11 _{0.25}	91.12 _{0.13}	90.64 _{0.05}	84.01 _{0.10}	83.47

Table 1: Results on the GLUE benchmark with $BERT_{base}$, where tasks are ordered in ascending order of the training resources. We conduct three groups of task transferability experiments on RTE and one resource scalability experiment on MNLI. We report the average fine-tuned parameters of *per-task* AUTOPEFT, where we conduct additional *per-task* searches on MRPC, STS-B, and CoLA, and take best-found configurations for the remaining tasks. We report Spearman’s Correlation for STS-B, Matthew’s Correlation for CoLA, and accuracy for all other tasks, where we report the matched accuracy for MNLI. The percentage of parameters is computed as a ratio of the number of additional parameters to the pretrained parameters. We reproduce all baselines and report the mean and standard deviation of all results for 5 random seeds. The **best**, second-best, and third-best results are marked in bold fonts and ranked by colour.

RoBERTa_{large} (Liu et al., 2019b) show findings that are consistent to the ones $BERT_{base}$, and are included in Table 3 in the appendix. We report the setup for each PEFT module and the detailed training scheme in §A.

5 Results and Discussion

Transferability of Configurations across Tasks.

The main results are summarized in Table 1. First, we analyze task transferability of AUTOPEFT-found configurations by running AUTOPEFT on the most low-resource and challenging task, RTE, followed by transferring the three best AUTOPEFT-found configurations to other tasks. First, we note that the parameter budget of the configuration AUTOPEFT^{RTE}_M is only 1.42%, while it shows considerable average gains over all the PEFT baselines on the RTE task, by a margin of at least 2%. The AUTOPEFT-found configuration also outperforms the full-model FT baseline on the RTE task by more than 1%. These results indicate the effectiveness of the AUTOPEFT framework in optimising both task performance and parameter efficiency. Transferring the RTE-based configurations to other tasks, we find that strong performance is maintained across the target tasks, with more benefits on the medium-resource tasks (MRPC, STS-B, CoLA), but the configuration remains competitive also for higher-resource tasks (e.g., QQP, MNLI).

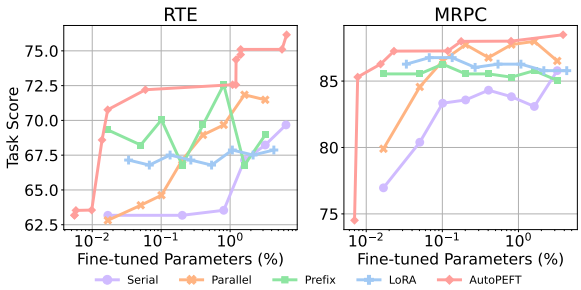


Figure 4: The Pareto front of the AUTOPEFT on tasks RTE and MRPC compared to baselines with $BERT_{base}$ in various settings of parameter budgets. We report the single-seed task score for each task following the settings in Table 1. The plots for STS-B, and CoLA, showing the same trends, are in Appendix §B.

When we assign a large parameter budget to the potential configurations, AUTOPEFT^{RTE}_L also shows a stronger transfer performance in high-resource tasks. This indicates that, as expected, the parameter capacity of the configuration is an important factor in transfer learning (Chen et al., 2022a). On average, the AUTOPEFT^{RTE}_M configuration shows a comparable fine-tuning performance, 83.19, to the full model FT, 83.15, by only updating 1.42% of parameters. With strong transferability across similar tasks, AUTOPEFT provides distinct advantages in parameter efficiency; the search algorithm itself coupled with transfer becomes more

sample-efficient within limited training resources.

Resource Scalability and Efficiency. We next ‘stress-test’ the ability of AUTOPEFT in a more challenging scenario with limited task training data, carrying out an experiment on the most high-resource MNLI task using only a small set of its training data. We randomly sample 1% of the original MNLI training data to train AUTOPEFT, and retain using the original dev set for evaluation.² We report AUTOPEFT_S^{MNLI} in Table 1 as the best-found configuration in this low-resource setting. It requires only 0.30% of fine-tuned parameters and shows the strong MNLI performance of 83.92%. In another efficiency-oriented test, we conduct configuration transfer in a radically parameter-efficient setup (training on the full RTE training set but with reduced parameter budget, and then transferring to other tasks; AUTOPEFT_S^{RTE} in Table 1). The main finding is that, while performance does decrease slightly as expected, strong task performance can still be achieved even with the parameter budget of 0.06% within this very efficient setup.

Per-Task Configuration Search. Finally, we conduct full-resource per-task AUTOPEFT searches, which naturally come with increased computational costs, for RTE, MRPC, STS-B, and CoLA, and then, for efficiency reasons, port the small set of best configurations to the remaining high-resource tasks: SST-2, QNLI, QQP, MNLI. In addition to the peak score on RTE, we observe gains on MRPC (87.16% to 87.45%) and CoLA (60.13% to 60.92%) over the best-performing PEFT baselines. We also observe gains over the transferred configuration AUTOPEFT_M^{RTE}. One interpretation of the results is that AUTOPEFT is strong at matching the intrinsic dimensionality of the low-resource downstream task to the capacity (i.e., parameter budget) of the PEFT modules, whereas full model FT performs better in high-resource scenarios, giving the largest capacity to capture the information in high-resource tasks.³ However, the per-task AUTOPEFT^{task} variant outperforms even full model FT by 0.3% while its parameter budget is only 1.4% of the full model per task.

Analysing the ‘Behaviour’ of Bayesian Optimi-

²With this setup, we effectively save 99% of training resources and the search framework becomes extremely fast even for high-resource datasets.

³Due to the richness of training resources in high-resource datasets, the results in these tasks are mostly saturated. Previous work shows that PEFT methods can only reach on-par performance to full model FT on those tasks.

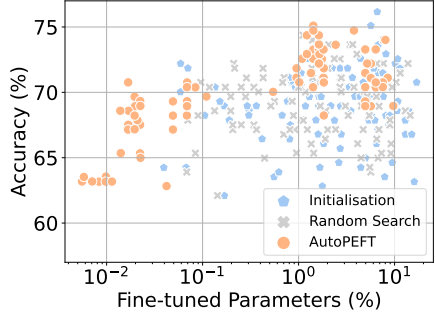


Figure 5: The distribution of AUTOPEFT-found configurations compared to the random search on RTE with a single random seed. We initialise the AUTOPEFT search with 100 runs of random sampling for initial explorations in the search space. We then conduct 100 runs of the AUTOPEFT with Bayesian optimisation.

sation. Figure 5 shows the distribution of AUTOPEFT-found configurations when we conduct its search experiment on RTE. Due to the greedy nature of our predefined acquisition function, we enforce the initialisation of our algorithm with a wide exploration of potential configurations. In the subsequent AUTOPEFT runs, it starts exploiting the best-found configurations while optimising towards the region with improved parameter efficiency, whereas the random search baseline keeps obtaining inefficient configurations in a lottery-ticket manner in the expensive region of parameters. It is observable that AUTOPEFT exploits the region with roughly 1.4% of parameters and finds configurations with further enhanced task performance from 74.4% to 75.1% of accuracy, which is also the architecture AUTOPEFT_M^{RTE} with the strongest transferability across tasks. We also include the best-found architecture within the initialisation stage as the AUTOPEFT_L^{RTE}, and our transferability experiments show that the AUTOPEFT-found architecture is more robust to the random initialisation of the neural network, outperforming the best random search baseline in the searched task by 0.7% with 5.2% less parameter cost.

Ablation of the Configuration Space. To provide a finer-grained analysis of factors that bring positive impact to AUTOPEFT, we ablate the AUTOPEFT search space from the full configuration space: 1) to the basic enumeration of the bottleneck size D_{SA} of the SA only (the ‘SA’ space). We then include the Transformer layer and the SA size together into the search space (the ‘SA-Layer’ space) to validate the usefulness of using layer selection as one configuration dimension. We can then also

Method	#Layers	Size D_{SA}	RTE Accuracy (%)
Serial Adapter	24	64	72.56 _{0.76}
Adaptable Adapter	13	128	73.36 _{0.80}
AdapterDrop	13	128	73.50 _{1.40}
AUTOPEFT _{Layer} ^{SA}	10	128	73.86 _{0.94}

Table 2: The results of AUTOPEFT to layer selection baselines with the same parameter budget on BERT_{large}. We report the Pfeiffer adapter for all 24 layers. We include the specialised AdapterDrop (Rücklé et al., 2021) that inserts SA for the last 13 layers. We report the AA_{uni} architecture (Moosavi et al., 2022) without its rational activation function with 13 selected layers. We run our AUTOPEFT with the comparable search space of 24 layers and the size of the Pfeiffer adapter.

expand the search space by adding another module (e.g., PA yields the ‘SA-PA-Layer’ space). Figure 6 plots the performance over the ‘ablated’ configuration spaces and over different parameter budgets. Several key findings emerge. First, combining multiple single PEFT modules has a positive impact on AUTOPEFT in general (cf., full AUTOPEFT versus ‘SA-PA-Layer’ versus ‘SA-Layer’). Relying on layer selection also brings benefits (cf., ‘SA’ versus ‘SA-Layer’). The comparison also indicates that leaving out some Transformer layers while increasing the capacity of the PEFT module is a straightforward method to improve the parameter efficiency and task performance of the PEFT module within a fixed parameter budget. Figure 6 suggests that AUTOPEFT can effectively operate over configuration spaces of different ‘granularity’.

We analyse the impact of each single PEFT module in more detail in Appendix §B.

Layer Selection. To further compare different layer selection approaches, we conduct a controlled experiment with the SA module on BERT_{large} (24 Transformer layers) under a predefined parameter budget. In Table 2, the simple AdapterDrop approach simply drops the adapters for the first 11 layers while doubling their bottleneck sizes, improving the RTE result by roughly 1%. Within the same architecture, we include the Adaptable Adapter with selected layers from switch learning, which has 3 and 10 layers from the first 12 and the other 12 layers, respectively. We show that AUTOPEFT outperforms all existing layer selection baselines by learning less activated adapter layers, leading to better parameter efficiency (12.5% fewer parameters in relative terms) and higher task performance. It indicates that selecting the best insertion

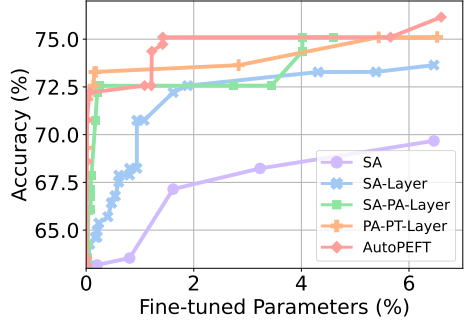


Figure 6: The performance of AUTOPEFT with ablation of search space on RTE with a single random seed on BERT_{base}. The SA results refer to the Pfeiffer adapter (Pfeiffer et al., 2020b) with an enumeration of its bottleneck size. For other search spaces, we report the Pareto front of AUTOPEFT-found configurations, where SA-PA-PT-Layer forms the search space of AUTOPEFT.

layer is non-trivial, and AUTOPEFT can learn the correlation between layers.

6 Conclusion

We proposed AUTOPEFT, a novel search framework for automatically configuring various PEFT modules in selective layers of pretrained language models. AUTOPEFT searches the optimal architecture via Bayesian optimisation with iterative evaluation and predicting the desired architecture given the configuration search space. The proposed multi-objective optimisation can produce a Pareto front of candidate architectures by simultaneously maximising the model performance and parameter efficiency. We demonstrated that AUTOPEFT-found architectures offer an effective trade-off between task performance and parameter efficiency, outperforming a variety of PEFT baselines.

Limitations

The proposed AUTOPEFT method is relatively expensive since it requires iterative optimisation by learning to optimise each explored configuration. While all intermediate configurations can be skipped without laying a burden on the final storage space, the intermediate computation cost becomes the main bottleneck of this approach. In this work, we alleviated this problem by (i) conducting the search with 1% of training resources for large datasets, and (ii) configuration transfer from low-resource tasks. The search itself can be seen as a one-time cost yielding a ‘permanent’ well-performing and shareable configuration for particu-

lar tasks. We plan to delve deeper into the related efficiency and computational tractability aspects in future work.

We have conducted extensive experiments on the search space that contains three representative PEFT modules. The AUTOPEFT framework is decoupled from the actual single PEFT modules: with further PEFT developments and new PEFT approaches, those may also get integrated into the AUTOPEFT framework in future work.

Acknowledgements

Xingchen Wan is supported by the Clarendon Scholarship at University of Oxford. The work has been supported in part by a personal Royal Society University Research Fellowship (no 221137; 2022-) awarded to Ivan Vulić.

References

Alan Ansell, Edoardo Ponti, Anna Korhonen, and Ivan Vulić. 2022. **Composable sparse fine-tuning for cross-lingual transfer**. In *Proceedings of the 60th Annual Meeting of the Association for Computational Linguistics (Volume 1: Long Papers)*, pages 1778–1796, Dublin, Ireland. Association for Computational Linguistics.

Maximilian Balandat, Brian Karrer, Daniel Jiang, Samuel Daulton, Ben Letham, Andrew G Wilson, and Eytan Bakshy. 2020. **Botorch: A framework for efficient monte-carlo bayesian optimization**. *Advances in neural information processing systems*, 33:21524–21538.

Elad Ben Zaken, Yoav Goldberg, and Shauli Ravfogel. 2022. **BitFit: Simple parameter-efficient fine-tuning for transformer-based masked language-models**. In *Proceedings of the 60th Annual Meeting of the Association for Computational Linguistics (Volume 2: Short Papers)*, pages 1–9, Dublin, Ireland. Association for Computational Linguistics.

Tom B. Brown, Benjamin Mann, Nick Ryder, Melanie Subbiah, Jared Kaplan, Prafulla Dhariwal, Arvind Neelakantan, Pranav Shyam, Girish Sastry, Amanda Askell, Sandhini Agarwal, Ariel Herbert-Voss, Gretchen Krueger, Tom Henighan, Rewon Child, Aditya Ramesh, Daniel M. Ziegler, Jeffrey Wu, Clemens Winter, Christopher Hesse, Mark Chen, Eric Sigler, Mateusz Litwin, Scott Gray, Benjamin Chess, Jack Clark, Christopher Berner, Sam McCandlish, Alec Radford, Ilya Sutskever, and Dario Amodei. 2020. **Language models are few-shot learners**. In *Advances in Neural Information Processing Systems 33: Annual Conference on Neural Information Processing Systems 2020, NeurIPS 2020, December 6-12, 2020, virtual*.

Guanzheng Chen, Fangyu Liu, Zaiqiao Meng, and Shangsong Liang. 2022a. **Revisiting parameter-efficient tuning: Are we really there yet?** In *Proceedings of the 2022 Conference on Empirical Methods in Natural Language Processing*, pages 2612–2626, Abu Dhabi, United Arab Emirates. Association for Computational Linguistics.

Shoufa Chen, Chongjian Ge, Zhan Tong, Jiangliu Wang, Yibing Song, Jue Wang, and Ping Luo. 2022b. **Adaptformer: Adapting vision transformers for scalable visual recognition**. In *Advances in Neural Information Processing Systems*.

Samuel Daulton, Maximilian Balandat, and Eytan Bakshy. 2021. **Parallel bayesian optimization of multiple noisy objectives with expected hypervolume improvement**. In *Advances in Neural Information Processing Systems 34: Annual Conference on Neural Information Processing Systems 2021, NeurIPS 2021, December 6-14, 2021, virtual*, pages 2187–2200.

Jacob Devlin, Ming-Wei Chang, Kenton Lee, and Kristina Toutanova. 2019. **BERT: Pre-training of deep bidirectional transformers for language understanding**. In *Proceedings of the 2019 Conference of the North American Chapter of the Association for Computational Linguistics: Human Language Technologies, Volume 1 (Long and Short Papers)*, pages 4171–4186, Minneapolis, Minnesota. Association for Computational Linguistics.

Xuanyi Dong and Yi Yang. 2020. **Nas-bench-201: Extending the scope of reproducible neural architecture search**. In *8th International Conference on Learning Representations, ICLR 2020, Addis Ababa, Ethiopia, April 26-30, 2020*.

Thomas Elsken, Jan Hendrik Metzen, and Frank Hutter. 2019. **Neural architecture search: A survey**. *The Journal of Machine Learning Research*, 20(1):1997–2017.

David Eriksson, Pierce I-Jen Chuang, Samuel Daulton, Peng Xia, Akshat Shrivastava, Arun Babu, Shicong Zhao, Ahmed A Aly, Ganesh Venkatesh, and Maximilian Balandat. 2021. **Latency-aware neural architecture search with multi-objective bayesian optimization**. In *8th ICML Workshop on Automated Machine Learning (AutoML)*.

David Eriksson and Martin Jankowiak. 2021. **High-dimensional bayesian optimization with sparse axis-aligned subspaces**. In *Uncertainty in Artificial Intelligence*, pages 493–503. PMLR.

Peter I. Frazier. 2018. **A tutorial on bayesian optimization**. *CoRR*, abs/1807.02811.

Roman Garnett. 2023. *Bayesian Optimization*. Cambridge University Press.

Demi Guo, Alexander Rush, and Yoon Kim. 2021. **Parameter-efficient transfer learning with diff pruning**. In *Proceedings of the 59th Annual Meeting of*

the Association for Computational Linguistics and the 11th International Joint Conference on Natural Language Processing (Volume 1: Long Papers), pages 4884–4896, Online. Association for Computational Linguistics.

Junxian He, Chunting Zhou, Xuezhe Ma, Taylor Berg-Kirkpatrick, and Graham Neubig. 2022. Towards a unified view of parameter-efficient transfer learning. In *The Tenth International Conference on Learning Representations, ICLR 2022, Virtual Event, April 25-29, 2022*.

Matthew D Hoffman, Andrew Gelman, et al. 2014. The no-u-turn sampler: adaptively setting path lengths in hamiltonian monte carlo. *J. Mach. Learn. Res.*, 15(1):1593–1623.

Neil Houlsby, Andrei Giurgiu, Stanislaw Jastrzebski, Bruna Morrone, Quentin de Laroussilhe, Andrea Gesmundo, Mona Attariyan, and Sylvain Gelly. 2019. Parameter-efficient transfer learning for NLP. In *Proceedings of the 36th International Conference on Machine Learning, ICML 2019, 9-15 June 2019, Long Beach, California, USA*, pages 2790–2799.

Edward J. Hu, Yelong Shen, Phillip Wallis, Zeyuan Allen-Zhu, Yuanzhi Li, Shean Wang, Lu Wang, and Weizhu Chen. 2022a. Lora: Low-rank adaptation of large language models. In *The Tenth International Conference on Learning Representations, ICLR 2022, Virtual Event, April 25-29, 2022*.

Shengding Hu, Zhen Zhang, Ning Ding, Yadao Wang, Yasheng Wang, Zhiyuan Liu, and Maosong Sun. 2022b. Sparse structure search for delta tuning. In *Advances in Neural Information Processing Systems*.

Sergio Izquierdo, Julia Guerrero-Viu, Sven Hauns, Guilherme Miotto, Simon Schrödi, André Biedenkapp, Thomas Elsken, Difan Deng, Marius Lindauer, and Frank Hutter. 2021. Bag of baselines for multi-objective joint neural architecture search and hyperparameter optimization. In *8th ICML Workshop on Automated Machine Learning (AutoML)*.

Kirthevasan Kandasamy, Willie Neiswanger, Jeff Schneider, Barnabás Póczos, and Eric P. Xing. 2018. Neural architecture search with bayesian optimisation and optimal transport. In *Advances in Neural Information Processing Systems 31: Annual Conference on Neural Information Processing Systems 2018, NeurIPS 2018, December 3-8, 2018, Montréal, Canada*, pages 2020–2029.

Brian Lester, Rami Al-Rfou, and Noah Constant. 2021. The power of scale for parameter-efficient prompt tuning. In *Proceedings of the 2021 Conference on Empirical Methods in Natural Language Processing*, pages 3045–3059, Online and Punta Cana, Dominican Republic. Association for Computational Linguistics.

Liam Li and Ameet Talwalkar. 2019. Random search and reproducibility for neural architecture search. In *Proceedings of the Thirty-Fifth Conference on Uncertainty in Artificial Intelligence, UAI 2019, Tel Aviv, Israel, July 22-25, 2019*, pages 367–377.

Xiang Lisa Li and Percy Liang. 2021. Prefix-tuning: Optimizing continuous prompts for generation. In *Proceedings of the 59th Annual Meeting of the Association for Computational Linguistics and the 11th International Joint Conference on Natural Language Processing (Volume 1: Long Papers)*, pages 4582–4597, Online. Association for Computational Linguistics.

Hanxiao Liu, Karen Simonyan, and Yiming Yang. 2019a. DARTS: differentiable architecture search. In *7th International Conference on Learning Representations, ICLR 2019, New Orleans, LA, USA, May 6-9, 2019*.

Haokun Liu, Derek Tam, Muqeeth Mohammed, Jay Mohta, Tenghao Huang, Mohit Bansal, and Colin Raffel. 2022. Few-shot parameter-efficient fine-tuning is better and cheaper than in-context learning. In *Advances in Neural Information Processing Systems*.

Yinhan Liu, Myle Ott, Naman Goyal, Jingfei Du, Mandar Joshi, Danqi Chen, Omer Levy, Mike Lewis, Luke Zettlemoyer, and Veselin Stoyanov. 2019b. Roberta: A robustly optimized BERT pretraining approach. *CoRR*, abs/1907.11692.

Rabeeh Karimi Mahabadi, James Henderson, and Sebastian Ruder. 2021. Compacter: Efficient low-rank hypercomplex adapter layers. In *Advances in Neural Information Processing Systems 34: Annual Conference on Neural Information Processing Systems 2021, NeurIPS 2021, December 6-14, 2021, virtual*, pages 1022–1035.

Yuning Mao, Lambert Mathias, Rui Hou, Amjad Almahairi, Hao Ma, Jiawei Han, Scott Yih, and Madian Khabsa. 2022. UniPELT: A unified framework for parameter-efficient language model tuning. In *Proceedings of the 60th Annual Meeting of the Association for Computational Linguistics (Volume 1: Long Papers)*, pages 6253–6264, Dublin, Ireland. Association for Computational Linguistics.

Nafise Moosavi, Quentin Delfosse, Kristian Kersting, and Iryna Gurevych. 2022. Adaptable adapters. In *Proceedings of the 2022 Conference of the North American Chapter of the Association for Computational Linguistics: Human Language Technologies*, pages 3742–3753, Seattle, United States. Association for Computational Linguistics.

Jonas Pfeiffer, Naman Goyal, Xi Lin, Xian Li, James Cross, Sebastian Riedel, and Mikel Artetxe. 2022. Lifting the curse of multilinguality by pre-training modular transformers. In *Proceedings of the 2022 Conference of the North American Chapter of the Association for Computational Linguistics: Human*

Language Technologies, pages 3479–3495, Seattle, United States. Association for Computational Linguistics.

Jonas Pfeiffer, Andreas Rücklé, Clifton Poth, Aishwarya Kamath, Ivan Vulić, Sebastian Ruder, Kyunghyun Cho, and Iryna Gurevych. 2020a. **AdapterHub: A framework for adapting transformers.** In *Proceedings of the 2020 Conference on Empirical Methods in Natural Language Processing: System Demonstrations*, pages 46–54, Online. Association for Computational Linguistics.

Jonas Pfeiffer, Ivan Vulić, Iryna Gurevych, and Sebastian Ruder. 2020b. **MAD-X: An Adapter-Based Framework for Multi-Task Cross-Lingual Transfer.** In *Proceedings of the 2020 Conference on Empirical Methods in Natural Language Processing (EMNLP)*, pages 7654–7673, Online. Association for Computational Linguistics.

Colin Raffel, Noam Shazeer, Adam Roberts, Katherine Lee, Sharan Narang, Michael Matena, Yanqi Zhou, Wei Li, and Peter J. Liu. 2020. **Exploring the limits of transfer learning with a unified text-to-text transformer.** *J. Mach. Learn. Res.*, 21:140:1–140:67.

Pengzhen Ren, Yun Xiao, Xiaojun Chang, Po-Yao Huang, Zhihui Li, Xiaojiang Chen, and Xin Wang. 2021. **A comprehensive survey of neural architecture search: Challenges and solutions.** *ACM Computing Surveys (CSUR)*, 54(4):1–34.

Bin Xin Ru, Xingchen Wan, Xiaowen Dong, and Michael A. Osborne. 2021. **Interpretable neural architecture search via bayesian optimisation with weisfeiler-lehman kernels.** In *9th International Conference on Learning Representations, ICLR 2021, Virtual Event, Austria, May 3-7, 2021*.

Robin Ru, Pedro M. Esperança, and Fabio Maria Carucci. 2020. **Neural architecture generator optimization.** In *Advances in Neural Information Processing Systems 33: Annual Conference on Neural Information Processing Systems 2020, NeurIPS 2020, December 6-12, 2020, virtual*.

Andreas Rücklé, Gregor Geigle, Max Glockner, Tilman Beck, Jonas Pfeiffer, Nils Reimers, and Iryna Gurevych. 2021. **AdapterDrop: On the efficiency of adapters in transformers.** In *Proceedings of the 2021 Conference on Empirical Methods in Natural Language Processing*, pages 7930–7946, Online and Punta Cana, Dominican Republic. Association for Computational Linguistics.

Victor Sanh, Albert Webson, Colin Raffel, Stephen Bach, Lintang Sutawika, Zaid Alyafeai, Antoine Chaffin, Arnaud Stiegler, Arun Raja, Manan Dey, M Saiful Bari, Canwen Xu, Urmish Thakker, Shanya Sharma Sharma, Eliza Szczęsła, Taewoon Kim, Gunjan Chhablani, Nihal V. Nayak, Debajyoti Datta, Jonathan Chang, Mike Tian-Jian Jiang, Han Wang, Matteo Manica, Sheng Shen, Zheng Xin Yong, Harshit Pandey, Rachel Bawden, Thomas Wang, Trishala Neeraj, Jos Rozen, Abheesh Sharma, Andrea Santilli, Thibault Févry, Jason Alan Fries, Ryan Teehan, Teven Le Scao, Stella Biderman, Leo Gao, Thomas Wolf, and Alexander M. Rush. 2022. **Multitask prompted training enables zero-shot task generalization.** In *The Tenth International Conference on Learning Representations, ICLR 2022, Virtual Event, April 25-29, 2022*.

Jasper Snoek, Hugo Larochelle, and Ryan P. Adams. 2012. **Practical bayesian optimization of machine learning algorithms.** In *Advances in Neural Information Processing Systems 25: 26th Annual Conference on Neural Information Processing Systems 2012. Proceedings of a meeting held December 3-6, 2012, Lake Tahoe, Nevada, United States*, pages 2960–2968.

Yi-Lin Sung, Varun Nair, and Colin Raffel. 2021. **Training neural networks with fixed sparse masks.** In *Advances in Neural Information Processing Systems 34: Annual Conference on Neural Information Processing Systems 2021, NeurIPS 2021, December 6-14, 2021, virtual*, pages 24193–24205.

Ian Tenney, Dipanjan Das, and Ellie Pavlick. 2019. **BERT rediscovers the classical NLP pipeline.** In *Proceedings of the 57th Annual Meeting of the Association for Computational Linguistics*, pages 4593–4601, Florence, Italy. Association for Computational Linguistics.

Ivan Vulić, Edoardo Maria Ponti, Robert Litschko, Goran Glavaš, and Anna Korhonen. 2020. **Probing pretrained language models for lexical semantics.** In *Proceedings of the 2020 Conference on Empirical Methods in Natural Language Processing (EMNLP)*, pages 7222–7240, Online. Association for Computational Linguistics.

Xingchen Wan, Vu Nguyen, Huong Ha, Binxin Ru, Cong Lu, and Michael A Osborne. 2021. **Think global and act local: Bayesian optimisation over high-dimensional categorical and mixed search spaces.** In *International Conference on Machine Learning*, pages 10663–10674. PMLR.

Xingchen Wan, Binxin Ru, Pedro M. Esperança, and Zhenguo Li. 2022. **On redundancy and diversity in cell-based neural architecture search.** In *The Tenth International Conference on Learning Representations, ICLR 2022, Virtual Event, April 25-29, 2022*. OpenReview.net.

Alex Wang, Amanpreet Singh, Julian Michael, Felix Hill, Omer Levy, and Samuel Bowman. 2018. **GLUE: A multi-task benchmark and analysis platform for natural language understanding.** In *Proceedings of the 2018 EMNLP Workshop BlackboxNLP: Analyzing and Interpreting Neural Networks for NLP*, pages 353–355, Brussels, Belgium. Association for Computational Linguistics.

Yaqing Wang, Sahaj Agarwal, Subhabrata Mukherjee, Xiaodong Liu, Jing Gao, Ahmed Hassan Awadallah

lah, and Jianfeng Gao. 2022. Adamix: Mixture-of-adaptations for parameter-efficient model tuning. In *Proceedings of the 2022 Conference on Empirical Methods in Natural Language Processing*, pages 5744–5760, Abu Dhabi, United Arab Emirates. Association for Computational Linguistics.

Colin White, Willie Neiswanger, and Yash Savani. 2021a. **BANANAS**: bayesian optimization with neural architectures for neural architecture search. In *Thirty-Fifth AAAI Conference on Artificial Intelligence, AAAI 2021, Thirty-Third Conference on Innovative Applications of Artificial Intelligence, IAAI 2021, The Eleventh Symposium on Educational Advances in Artificial Intelligence, EAAI 2021, Virtual Event, February 2-9, 2021*, pages 10293–10301.

Colin White, Arber Zela, Robin Ru, Yang Liu, and Frank Hutter. 2021b. How powerful are performance predictors in neural architecture search? In *Advances in Neural Information Processing Systems 34: Annual Conference on Neural Information Processing Systems 2021, NeurIPS 2021, December 6-14, 2021, virtual*, pages 28454–28469.

Antoine Yang, Pedro M. Esperança, and Fabio Maria Carlucci. 2020. **NAS evaluation is frustratingly hard**. In *8th International Conference on Learning Representations, ICLR 2020, Addis Ababa, Ethiopia, April 26-30, 2020*.

Mengjie Zhao, Tao Lin, Fei Mi, Martin Jaggi, and Hinrich Schütze. 2020. **Masking as an efficient alternative to finetuning for pretrained language models**. In *Proceedings of the 2020 Conference on Empirical Methods in Natural Language Processing (EMNLP)*, pages 2226–2241, Online. Association for Computational Linguistics.

Barret Zoph and Quoc V. Le. 2017. **Neural architecture search with reinforcement learning**. In *5th International Conference on Learning Representations, ICLR 2017, Toulon, France, April 24-26, 2017, Conference Track Proceedings*.

A Supplemental Material: Technical Details

PEFT Modules: Architectures and Setup. We implement the serial adapter architecture (SA) following the setup of Pfeiffer et al. (2020b). The parallel adapter (PA) architecture is the same as the one proposed by He et al. (2022), where a scaling factor of 4 is implemented in all PA experiments. The prefix-tuning (PT) architecture has an intermediate MLP with a bottleneck size of 800, which is trained the same way as in the original work (Li and Liang, 2021). We also use the default setting for LoRA with a scaling of 8 and a rank of 8. We reproduce the experimental results with the reported setup of the MAM adapter He et al. (2022) and

UniPELT (Mao et al., 2022). We reproduce the AdaMix results with the reported hyperparameter setup from the original work (Wang et al., 2022) in 20 epochs. In the experiments of Figure 4, we control the bottleneck size D_{SA} and D_{PA} for SA and PA baselines, respectively, while keeping other setups unchanged to discover their performance across the parameter budget. Similarly, we control the prefix length L_{PT} for prefix-tuning and the rank r of LoRA without changing other setups.

Training Details. Following previous work (Pfeiffer et al., 2020b), we use a recommended learning rate of 1e-4 for all PEFT experiments. In RoBERTa_{large} experiments, we report the RTE results with a learning rate of 2e-5 for AUTOPEFT^{MRPC} and AUTOPEFT^{CoLA}; 1e-4 for AUTOPEFT^{RTE}. We use the learning rate of 2e-5 for full model FT according to Mao et al. (2022). We use the batch size of 32 and 16 for all BERT and RoBERTa experiments, respectively. The optimiser settings for each PEFT module follow the default settings in AdapterHub (Pfeiffer et al., 2020a).

AUTOPEFT Search Setup. We implement the BO algorithm in BoTorch (Balandat et al., 2020). We use the Matern 5/2 kernel as the covariance function, and for the Monte Carlo sampling settings of SAAS-BO (Eriksson and Jankowiak, 2021), we use a warm-up step of 256, the number of samples to retain as 128, and thinning as 16. For the optimisation of the acquisition function, to adapt to the discrete setup, we use a local search method similar to previous literature involving similar setup (Wan et al., 2021; Eriksson et al., 2021): at each search iteration (after the initial randomly sampled points), we collect the *Pareto-optimal* architectures up to this point. From this collection of Pareto-optimal architectures, we perform a local search by evaluating the acquisition function values of their neighbours, and move the current point to a neighbour with a higher acquisition function value and this process is repeated until convergence (which is a local minimum in terms of acquisition function), or 100 evaluations in acquisition function value are reached. At each search iteration, we restart this process 10 times and select the top candidate for the query (in this case, fine-tuning) for the next iteration. For all BO experiments, we use 200 total evaluations; given the noisy nature of the problem, we use a relatively large number of random initialisation points (100) to ensure that the search results

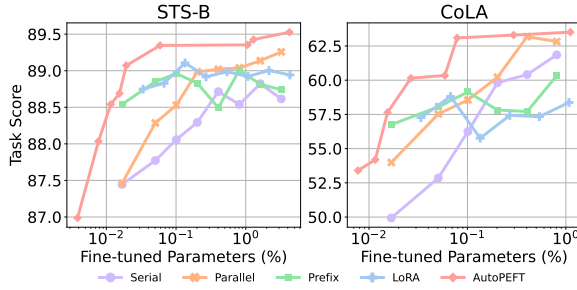


Figure 7: The Pareto front of the AUTOPEFT framework on tasks STS-B and CoLA compared to baselines with $\text{BERT}_{\text{base}}$ in various settings of parameter budgets. We report the single-seed task score for each task following the settings in Table 1.

are not overly sensitive to initialisation. We use the same hyperparameter settings as described for all experiments conducted in this paper.

Calculation of Fine-tuned Parameters. The uncased $\text{BERT}_{\text{base}}$ model (109M) has 12 Transformer layers with a hidden dimension size of 768. The uncased $\text{BERT}_{\text{large}}$ model (335M) and RoBERTa_{large} (355M) both have 24 layers with a hidden dimension size of 1,024. For both SA and PA, their fine-tuned parameters are computed by $2 \times D_{\text{adapter}} \times D_{\text{h}} \times |l|$, where D_{h} represents the corresponding hidden dimension of the selected model, and $|l|$ refers to the total selected number of insertion layers. Similarly, we calculate the fine-tuned parameters of PT by $2 \times L_{\text{PT}} \times D_{\text{h}} \times |l|$. Thus, the number of fine-tuned parameters of the AUTOPEFT-found configurations is a summation of individual PEFT modules’ parameters. We report the default fine-tuned parameters for the remaining PEFT modules as defined in their original papers.

B Search Space and Discovered Architectures

Impact of Single PEFT Modules within AUTOPEFT and Other Side Analyses. We provide a more detailed analysis of the behaviour of AUTOPEFT by inspecting the Pareto front of AUTOPEFT-found configurations when we ablate each PEFT module into the search space, as plotted in Figure 6. After combining the serial adapter with the parallel adapter, the upper bound of performance is improved by more than 1%. We consider the gain here leverages the capacity of multiple heterogeneous PEFT modules as a mixture-of-experts while providing a more efficient adaptation by up-

dating both bias-influenced hidden states and the original states according to Eq. 3. We recall that prefix-tuning stabilises its learning with an intermediate reparametrization network, which is dropped in the inference stage. Therefore, at the cost of the increased training parameters, prefix-tuning is one of the most parameter-efficient approaches. Consequently, we notice that incorporating prefix-tuning into the search space further improves the overall parameter efficiency (4% to 1.4%) of the AUTOPEFT-found configuration. Due to the parameter efficiency of each single PEFT module, it also explains the distribution of the parameter budget for each PEFT module in the learned configurations. We also analyse the learned configurations in terms of the selected layers over different parameter scales in Table 5. They show a common trend in selecting the higher Transformer layers to insert the PEFT modules, which coincides with previous findings that the higher layer contains richer task-specific representations, and introducing PEFT modules to these layers is more efficient than other layers. With the AUTOPEFT-found configurations reported in Table 5, we hope future PEFT research and applications can benefit from the architecture design similar to AUTOPEFT_M^{RTE} that we find the most transferable across tasks.

Method	#Param.	RTE	MRPC	STS-B	CoLA	SST-2	QNLI	Avg.
Fine-tune [†]	100%	86.6	90.9	92.4	68.0	96.4	94.7	88.2
LoRA [‡]	0.22%	85.2	90.2	92.3	68.2	96.2	94.8	87.8
Serial	0.89%	84.8	90.2	92.0	66.8	96.3	94.7	87.5
AUTOPEFT ^{RTE} _S	0.03%	88.1	89.5	92.3	62.7	96.0	94.6	87.2
AUTOPEFT ^{MRPC} _S	0.25%	86.6	92.2	92.2	66.6	96.2	94.6	88.1
AUTOPEFT ^{CoLA} _M	2.36%	85.9	90.0	91.8	70.6	96.8	94.6	88.3
AUTOPEFT ^{RTE} _L	9.41%	89.5	88.5	91.6	65.6	95.9	94.6	87.6
AUTOPEFT ^{task} _{Avg.}	0.88%	88.1	92.2	92.4	70.6	96.8	94.6	89.1

Table 3: Experimental results on the GLUE benchmark with RoBERTa_{large}. We report the full model fine-tuning[†] results from Liu et al. (2019b) with Pearson correlation for STS-B and Matthew’s correlation for CoLA. We include the LoRA[‡] module performance from Hu et al. (2022a). We report single-seed results for the experiments and exclude QQP and MNLI tasks due to the large computation cost of RoBERTa_{large}. Similar to Table 1, we conduct *per-task* search experiments on RTE, MRPC, STS-B, and CoLA, transferring best-found configurations to the remaining tasks. In addition to the transfer experiment from RTE, we also report transfer performance from MRPC and CoLA tasks with significantly different parameter budgets. All reported results are from the configurations listed in Table 7. The **best**, **second-best**, and **third-best** results are marked in bold fonts and ranked by colour.

Model	Insertion Layer $\{l_i\}$	Module	Size
BERT _{base}	1, 2, 3, 4, 5, 6,	Serial Adapter D_{SA}	0, 1, 3, 6, 12, 24, 48, 96, 192, 384, 768
	7, 8, 9, 10, 11, 12	Parallel Adapter D_{PA}	0, 1, 3, 6, 12, 24, 48, 96, 192, 384, 768
		Prefix-Tuning L_{PT}	0, 1, 3, 6, 12, 24, 48, 96, 192, 384, 768
BERT/RoBERTa _{large}	1, 2, 3, 4, 5, 6, 7, 8, 9, 10, 11, 12,	Serial Adapter D_{SA}	0, 1, 2, 4, 8, 16, 32, 64, 128, 256, 512, 1024
	13, 14, 15, 16, 17, 18, 19, 20, 21, 22, 23, 24	Parallel Adapter D_{PA}	0, 1, 2, 4, 8, 16, 32, 64, 128, 256, 512, 1024
		Prefix-Tuning L_{PT}	0, 1, 2, 4, 8, 16, 32, 64, 128, 256, 512, 1024

Table 4: The search space of the AUTOPEFT. Each insertion layer has a Boolean decision for inserting the PEFT modules. The 0 size of submodules indicates that we exclude the corresponding submodule from the configuration. The total number of configurations for BERT_{base}: $2^{12} \times 11 \times 11 \times 11 \approx 5 \times 10^6$ and for BERT/RoBERTa_{large}: $2^{24} \times 12 \times 12 \times 12 \approx 3 \times 10^{10}$.

Task	#Param.	Search Space	Configuration	Submodule	Configuration
RTE	0.06%	Layer l_i	3, 4, 6, 8, 9, 11	Serial Adapter D_{SA} Parallel Adapter D_{PA} Prefix-Tuning L_{PT}	3 1 3
RTE	1.42%	Layer l_i	2, 5, 6, 7, 8, 9, 10	Serial Adapter D_{SA} Parallel Adapter D_{PA} Prefix-Tuning L_{PT}	96 48 1
RTE	6.60%	Layer l_i	3, 4, 6, 7, 8, 9, 10	Serial Adapter D_{SA} Parallel Adapter D_{PA} Prefix-Tuning L_{PT}	384 192 96
MRPC	3.86%	Layer l_i	2, 3, 6, 7, 9, 10, 11	Serial Adapter D_{SA} Parallel Adapter D_{PA} Prefix-Tuning L_{PT}	6 384 3
STS-B	1.06%	Layer l_i	2, 5, 7, 8, 9, 11	Serial Adapter D_{SA} Parallel Adapter D_{PA} Prefix-Tuning L_{PT}	96 6 24
CoLA	0.29%	Layer l_i	3, 4, 8, 9, 10	Serial Adapter D_{SA} Parallel Adapter D_{PA} Prefix-Tuning L_{PT}	12 24 6
MNLI	0.30%	Layer l_i	3, 6, 7, 8, 9, 11, 12	Serial Adapter D_{SA} Parallel Adapter D_{PA} Prefix-Tuning L_{PT}	24 6 1

Table 5: The AUTOPEFT-found configurations reported in Table 1 using BERT_{base}. The average of fine-tuned parameters (%) of AUTOPEFT_{Avg}^{task} is calculated by $(1.42 + 3.86 + 1.06 + 0.29 + 1.42 + 0.30 + 1.42 + 1.42) / 8 = 1.40$, where we transfer the best-found AUTOPEFT_M^{RTE} to SST-2, QQP, and MNLI as their best *per-task* configurations for achieving the best trade-off between task performance and efficiency.

Task	#Param.	Search Space	Configuration	Submodule	Configuration
RTE	0.78%	Layer l_i	2, 6, 8, 11, 14, 15, 16, 17, 21, 23	Serial Adapter D_{SA}	128

Table 6: The AUTOPEFT-found configurations reported in Table 2 using BERT_{large}.

Task	#Param.	Search Space	Configuration	Submodule	Configuration
RTE	0.03%	Layer l_i	6, 10, 14, 15, 18, 19, 21, 23	Serial Adapter D_{SA} Parallel Adapter D_{PA} Prefix-Tuning L_{PT}	2 4 1
RTE	9.41%	Layer l_i	1, 2, 3, 4, 5, 7, 11, 12, 14, 15, 17, 19, 20, 21, 23	Serial Adapter D_{SA} Parallel Adapter D_{PA} Prefix-Tuning L_{PT}	64 1 1024
MRPC	0.25%	Layer l_i	1, 2, 4, 5, 6, 8, 9, 10, 11, 13, 14, 16, 17, 21, 22, 23, 24	Serial Adapter D_{SA} Parallel Adapter D_{PA} Prefix-Tuning L_{PT}	8 2 16
STS-B	0.25%	Layer l_i	1, 2, 4, 5, 6, 7, 8, 9, 10, 11, 13, 14, 16, 17, 21, 22, 24	Serial Adapter D_{SA} Parallel Adapter D_{PA} Prefix-Tuning L_{PT}	8 2 16
CoLA	2.36%	Layer l_i	1, 5, 6, 8, 9, 10, 13, 14, 15, 19, 21, 22, 23, 24	Serial Adapter D_{SA} Parallel Adapter D_{PA} Prefix-Tuning L_{PT}	256 32 4

Table 7: The AUTOPEFT-found configurations reported in Table 3 using RoBERTa_{large}. The average of fine-tuned parameters (%) of AUTOPEFT_{Avg}^{task} is calculated by $(0.03 + 0.25 + 0.25 + 2.36 + 2.36 + 0.03) / 6 = 0.88$, where we transfer the best-found AUTOPEFT_M^{CoLA} to SST-2 and AUTOPEFT_S^{RTE} to QNLI as their best *per-task* configurations for achieving the best trade-off between performance and efficiency.